

Reduced spin-down rate of PSR J0738–4042 explained as due to an asteroid disruption event

Yong-Bo Yu and Yong-Feng Huang

Department of Astronomy, Nanjing University, Nanjing 210046, China; hyf@nju.edu.cn
Key Laboratory of Modern Astronomy and Astrophysics (Nanjing University), Ministry of Education, Nanjing 210046, China

Received 2015 August 15; accepted 2015 November 12

Abstract Long term observations by Brook et al. reveal that the derivative of rotational frequency of PSR J0738–4042 changed abruptly in 2005. Originally, the spin-down rate was relatively stable, with the rotational frequency derivative being $-1.14 \times 10^{-14} \text{ s}^{-2}$. After September 2005, the derivative began to rise. About 1000 days later, it arrived at another relatively stable value of about $-0.98 \times 10^{-14} \text{ s}^{-2}$, indicating that the pulsar is spinning-down relatively slowly. To explain the observed change in spin-down rate, we resort to an asteroid disrupted by PSR J0738–4042. In our model, the orbital angular momentum of the asteroid is assumed to be parallel to that of the rotating pulsar, so that the pronounced reduction in the spin-down rate can be naturally explained as due to the transfer of angular momentum from the disrupted material to the central pulsar. The derived magnetospheric radius is about $7.0 \times 10^9 \text{ cm}$, which is smaller than the tidal disruption radius ($8.7 \times 10^{10} \text{ cm}$). Our model is self-consistent. It is shown that the variability in the spin-down rate of PSR J0738–4042 can be quantitatively accounted for by accretion from the asteroid disrupted by the central pulsar.

Key words: stars: neutron — planet-star interactions — pulsars: individual (PSR J0738–4042)

1 INTRODUCTION

Pulsars are widely believed to be fast rotating neutron stars, which are compact objects with typical radius $R \sim 10^6 \text{ cm}$ and mass $M \sim 1.4 M_{\odot}$. Pulsars usually have relatively stable pulse profiles and rotational periods, due to which they can even be used as unique high-precision clocks in experimental astrophysics. However, sometimes there are some timing variabilities observed in pulsars, such as glitches (Wang et al. 2000; Yuan et al. 2010; Espinoza et al. 2011; Manchester & Hobbs 2011; Yu et al. 2013), micro-glitches (Cognard & Backer 2004; Mandal et al. 2009), changes in the pulse profile (Rankin 1986; Burgay et al. 2005; Poutanen et al. 2009; Karastergiou et al. 2011; Bilous et al. 2014), pulse nulling (Deich et al. 1986; Rankin & Wright 2008; Jones 2011; Li et al. 2012), and pulse drifting (Backer 1973; Page 1973; Ruderman 1976; Esamdin et al. 2005; Jones 2014).

Neutron star glitches, characterized by a sudden increase and gradual relaxation of rotational frequency, are very interesting astrophysical phenomena and have been observed from many normal pulsars and magnetars (Kaspi et al. 2000; Dib et al. 2009; Livingstone et al. 2010; Gavriil et al. 2011), where magnetars are a type of pulsar with dipole magnetic fields significantly stronger than $4.4 \times 10^{13} \text{ G}$ (Usov 1992; Duncan & Thompson 1992; Olausen &

Kaspi 2014). Usually, glitches are believed to be associated with sudden decoupling of the pinned vortex lines in the crustal neutron superfluid region (Anderson & Itoh 1975; Pines & Alpar 1985; Alpar & Baykal 2006; Warszawski & Melatos 2011; Haskell et al. 2012; Warszawski et al. 2012; Chamel 2013). In the normal steady state, the pinned superfluid is coupled to the rest of the neutron star. But when the pinned superfluid is decoupled due to continuously increasing rotation lag, the angular momentum of the fast-rotating interior superfluid component will be transferred to the outer solid crust, leading to an observed glitch. There are also some other models to explain the observed glitches, such as the platelet collapse model (Morley & Schmidt 1996), the superfluid r-mode instability mechanism (Glampedakis & Andersson 2009), the snowplow model (Seveso et al. 2012), and the starquake model (Zhou et al. 2014).

Anti-glitches have also been observed in pulsars, such as from 1E 2259+586 (Archibald et al. 2013) and 1E 1841-045 (Şaşmaz Muş et al. 2014). Anti-glitches could be generated by either an internal mechanism such as an impulsive angular momentum transfer between the superfluid region and the crust (Thompson et al. 2000), or an external mechanism such as a sudden twisting of the magnetic field lines (Lytikov 2013) or accretion of retrograde matter (Katz 2014; Ouyed et al. 2014). However, the anti-glitch

of the magnetar 1E 2259+586 was very special, associated with a hard X-ray burst, which strongly challenges traditional glitch theories. Huang & Geng (2014) proposed a completely different model to interpret this strange behavior. In their model, the sudden spin-down is explained as being induced by collision of a small solid body with the central magnetar. The associated hard X-ray burst and the decaying softer X-ray emission can be explained well.

Recently, a sudden change in the spin-down rate of PSR J0738–4042 was reported by Brook et al. (2014). The value of the spin-down rate was originally quite stable. But after September 2005, a significant reduction in the spin-down rate was observed. This abrupt change coincided with the appearance of a new component in the average pulse profile (Karastergiou et al. 2011). As these timing and emission properties cannot be explained by normal intrinsic pulsar processes, Brook et al. (2014) argued that they were generated by an external mechanism and invoked the process of an asteroid being disrupted by the central neutron star. However, we noticed that their calculations are not self-consistent. Here we show that accretion from tidally disrupted material is truly a possible explanation for the special behaviors observed in the spin-down rate and present a self-consistent calculation.

The structure of our paper is organized as follows. We summarize the observational facts of PSR J0738–4042 in Section 2. The asteroid disruption model, including the tidal disruption and accretion processes, are described in Section 3. We summarize our results in the final section with a brief discussion.

2 OBSERVATIONAL FACTS

PSR J0738–4042 is a radio-emitting neutron star with a rotational period of 0.375 s and spin-down evolution of $\dot{\nu} = -1.14 \times 10^{-14} \text{ s}^{-2}$ (Brook et al. 2014), where $\dot{\nu}$ is the time derivative of the rotational frequency ν , which is gradually decreasing due to magnetic dipole radiation. As the target of a long-term monitoring campaign, PSR J0738–4042 has been observed by researchers at the Hartebeesthoek Radio Astronomy Observatory in South Africa from September 1988. PSR J0738–4042 has also been observed by the Parkes radio telescope in Australia as part of the Parkes timing programme associated with Fermi observations since 2007 (Weltevrede et al. 2010). PSR J0738–4042 shares similar rotational properties with other isolated, middle-aged radio pulsars. The pulse profile and timing property of PSR J0738–4042 were originally stable, with $\dot{\nu} = -1.14 \times 10^{-14} \text{ s}^{-2}$ (see Fig. 1).

In Figure 1, since a smaller $\dot{\nu}$ value means the pulsar is spinning-down relatively quickly, we call this initial stage the Fast Spinning-Down Phase. However, from September 2005, a dramatic change in the spin-down rate occurred (Brook et al. 2014, also see Figure 1 for a schematic illustration). This change was accompanied by a new radio component that drifted on the leading edge of the pulse profile, which was first noted by Karastergiou et al. (2011). The value of $\dot{\nu}$ gradually rose to a peak value of

$-0.98 \times 10^{-14} \text{ s}^{-2}$ about 450 days after September 2005. The amplitude of this change in the spin-down rate is about $0.16 \times 10^{-14} \text{ s}^{-2}$. Note that there are also some small variabilities during the rising phase. As marked in Figure 1, we call this stage the First Pulse. After reaching the peak value, $\dot{\nu}$ began to drop slightly. In Figure 1, this stage is marked by “Drop.” After dropping to a value of $-1.08 \times 10^{-14} \text{ s}^{-2}$, another significant change in the spin-down rate began. The value of $\dot{\nu}$ rose back to $-1.0 \times 10^{-14} \text{ s}^{-2}$ in about 300 days. After some small turbulence, the spin-down rate finally arrived at another relatively stable phase, with a new value of $\dot{\nu} = -0.98 \times 10^{-14} \text{ s}^{-2}$ (Brook et al. 2014). We call this stage the Slowly Spinning-Down Phase, since a higher $\dot{\nu}$ value indicates that the pulsar is spinning-down relatively slowly.

As the change in the spin-down rate of PSR J0738–4042 is accompanied by an emergent radio component that drifts with respect to the rest of the pulse profile, normal intrinsic pulsar processes cannot explain these radio emissions and timing features. Brook et al. (2014) suggested that they are witnessing an encounter of the pulsar with an asteroid. Due to orbital perturbations and collisions, asteroids may migrate inwards and interact with the magnetosphere after being disrupted by the central pulsar, affecting the pulse profile and the rotational stability. According to Brook et al. (2014), the change in the spin-down rate was caused by mass supplied to the pulsar. However, when calculating the total accreted mass, they first related the reduction in the outflowing charge density to the change in the spin-down rate. Then they multiplied the reduced charge density by the speed of light, the polar cap area and the duration of the new spin-down state to get a mass of about $1.0 \times 10^{15} \text{ g}$. They pointed out that this value is the mass of the asteroid encountering the central pulsar. But in fact, the mass estimated by Brook et al. (2014) is the reduction in mass due to the total outflowing plasma above the polar caps. It cannot be regarded as the mass of the accreted material, which itself is a kind of inflow. Thus it is obvious that their interpretation and calculations are not self-consistent. In this paper, to explain the behavior of the spin-down rate of PSR J0738–4042, we reconsider the tidal disruption and accretion processes in detail and give a self-consistent model.

3 MODEL

Interestingly, Shannon et al. (2013) showed that the timing variabilities of PSR B1937+21 are consistent with the existence of an asteroid belt. Actually, planetary and disk systems have been confirmed in some neutron stars, such as PSR B1257+12 (Wolszczan 1994), PSR B1620-26 (Thorsett et al. 1999) and the magnetar 4U 0142+61 (Wang et al. 2006). The mechanism of collision between small bodies and neutron stars has also been widely used to interpret transient X/γ-ray events (van Buren 1981; Livio & Taam 1987; Zhang et al. 2000; Campana et al. 2011). To explain the pronounced change in the spin-down rate of PSR J0738–4042, we invoke a close encounter between

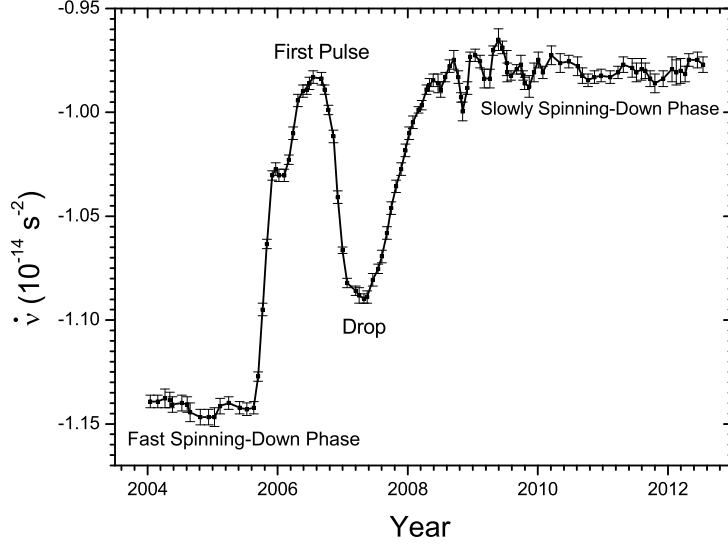


Fig. 1 A schematic illustration of the evolution of the rotational frequency derivative ($\dot{\nu}$) of PSR J0738–4042. The observational data are taken from Brook et al. (2014). See Brook et al. (2014) for a detailed plot.

an asteroid and the central pulsar. Since the spin-down rate reduced significantly (the $\dot{\nu}$ value increased, see Fig. 1) after September 2005, the orbital angular momentum of the asteroid is assumed to be parallel to that of PSR J0738–4042. In our framework, the asteroid will first be disrupted at the tidal disruption radius. After the disruption, some fraction of the disrupted material will be ejected at high speed, while the rest is bound to the central pulsar (Rees 1988). When the bound material moves around the central pulsar, the gaseous debris will be partially accreted onto the surface of the central pulsar, changing the emission and pulse profile signatures. Initially, the bound orbit is highly eccentric. As the material tends to stay in an orbit with the lowest energy for a given angular momentum, i.e. a circular orbit, the disrupted and bound debris will experience a process called orbital circularization. After orbital circularization occurs, a disk would be formed. From then on, the mass accretion rate tends to be somewhat constant before the exhaustion of material in the transient disk. We show that the observed behavior of the spin-down rate of PSR J0738–4042 can be well explained by the accretion processes at different stages.

3.1 Tidal Disruption and Initial Accretion

Due to strong gravitational force, an asteroid that comes too close to the pulsar will be broken up when approaching the tidal disruption radius given by (Hills 1975)

$$R_t \approx (6M/\pi\rho)^{1/3}, \quad (1)$$

where M is the pulsar mass and ρ is the characteristic density of the asteroid, which will be taken as 8 g cm^{-3} for a typical homogeneous iron-nickel body (Colgate &

Petschek 1981) for simplicity in our calculations. The tidal disruption radius is typically $R_t = 8.7 \times 10^{10} \text{ cm}$. After the disruption, some of the disrupted material will be bound to the central pulsar. In its first flyby, a small portion of the bound material will be accreted towards the central pulsar. During the accretion process, the infalling material will exert its own force to generate ram pressure. Because of the existence of a dipole magnetic field, there will also be magnetic pressure at any given radius. Equating the two pressures, we can obtain the Alfvén radius, which is also known as the magnetospheric radius, given by

$$r_m = \left(\frac{\mu^4}{GM\dot{m}^2} \right)^{1/7}, \quad (2)$$

where G is the gravitational constant and \dot{m} is the mass accretion rate. $\mu = B_0 R^3$ is the magnetic dipole moment of the pulsar and B_0 is the surface magnetic field, which can be estimated as

$$B_0 = 6.4 \times 10^{14} \left(\frac{P}{10 \text{ s}} \frac{\dot{P}}{10^{-11}} \right)^{1/2}, \quad (3)$$

$$G \approx 1.57 \times 10^{12} \text{ G},$$

by assuming all the rotational energy loss is due to magnetic dipole radiation, where P is the rotational period and \dot{P} is the derivative of the rotational period.

In our calculations, the disrupted material is assumed to be accreted and adheres to the central pulsar from the magnetospheric radius. Conservation of angular momentum then leads to

$$I \cdot 2\pi\nu + mVr_m = I \cdot 2\pi(\nu + \Delta\nu), \quad (4)$$

where I is the moment of inertia of the central pulsar, which is taken as a typical value of $I \sim 10^{45} \text{ g cm}^2$ (Pizzochero 2011; Hooker et al. 2015), and m is the mass of the accreted material. V is the velocity of the asteroid at the radius r_m , assumed to be $V = (2GM/r_m)^{1/2}$. Considering contributions from the material stress, as well as magnetic and viscous stresses, Ghosh & Lamb (1979b) calculated the accretion torque acting on a magnetic neutron star accreting matter from a disk in detail. They pointed out that an excellent approximation of the torque is given by the accreting material stress on a cylindrical surface S_1 located at the magnetospheric radius, since the viscous stress on S_1 is negligible by comparison (Ghosh & Lamb 1979a) while the magnetic stress has no component perpendicular to S_1 . Here, we assume that the change in angular momentum of PSR J0738–4042 is mainly due to the accreting material. Through some simple derivation we can further simplify Equation (4) to

$$\dot{m}(2GM r_m)^{1/2} = 2\pi I \cdot \Delta(\dot{\nu}). \quad (5)$$

To estimate the characteristic mass accretion rate, we first assume it to be constant. $\Delta(\dot{\nu})$ is taken as $0.16 \times 10^{-14} \text{ s}^{-2}$, which is determined from observational data (i.e., the difference of $\dot{\nu}$ in the Fast Spinning-Down Phase and in the First Pulse phase, see Fig. 1). For typical parameters of $M = 1.4 M_\odot$ and $R = 10^6 \text{ cm}$, the average mass accretion rate can be calculated as $\dot{m} = 6.0 \times 10^{12} \text{ g s}^{-1}$. In this case, the Alfvén radius can be estimated as $r_m = 7.0 \times 10^9 \text{ cm}$.

We argue that the First Pulse phase beginning from September 2005 in Figure 1 is due to the initial accretion of the gaseous debris in the first flyby after the disruption. Based on observations, there is a drop in the $\dot{\nu} - t$ diagram after the First Pulse, as shown in Figure 1. This is because, after passing the pericenter, the majority of the disrupted material will fly away from the central pulsar along a highly elliptical orbit. It will result in a decrease of the mass accretion rate, leading to a drop of $\dot{\nu}$. In our calculations, we assume the duration of the First Pulse, which is about 700 days, is the initial orbital period (T) of the bound debris. According to the formula $T = 2\pi \sqrt{\frac{a^3}{GM}}$, the semi-major axis a of the initial elliptical orbit can be calculated as $a = 2.6 \times 10^{13} \text{ cm}$, which is larger than the tidal disruption radius and the Alfvén radius, indicating that our calculations are self-consistent. There is also another timescale, the fall back timescale, which is the time for the bound debris to return to the pericenter (Ulmer 1999; Lu et al. 2006)

$$t_{\text{fb}} = \frac{2\pi R_p^3}{(GM)^{1/2} (2r)^{3/2}}, \quad (6)$$

where r is the radius of the asteroid and R_p is the pericenter distance. Actually, the fall back mechanism may also exist in the phenomenon of gamma-ray bursts (GRBs), which has been used to interpret significant X-ray rebrightenings observed in some GRB afterglows (Wu et al. 2013; Yu et al. 2015). As shown in Figure 1, the mass accretion rate should be constant at least up to 2012 - 2013,

which means that the fall back timescale is larger than six years. The asteroid radius has a lower limit corresponding to the total accreted mass in the six years with $\dot{m} = 6.0 \times 10^{12} \text{ g s}^{-1}$. Combining the lower limit of t_{fb} , the lower limit of the pericenter distance can be estimated as $R_p = 1.9 \times 10^{10} (m/10^{21} \text{ g})^{1/6} (t_{\text{fb}}/6 \text{ years})^{1/3} \text{ cm}$. Additionally, we assume that the accretion energy is released at the neutron star surface. Then the accretion luminosity is $L = \dot{m}c^2 = 4\pi R^2 \sigma_{\text{SB}} T^4$, where σ_{SB} is the Stefan-Boltzmann constant. The characteristic temperature of the radiation can be estimated as $T \approx 2 \times 10^6 \text{ K}$. The maximum power is radiated at photon energy $\varepsilon \sim k_B T \approx 170 \text{ eV}$, falling in the extreme ultraviolet band, where k_B is the Boltzmann constant.

3.2 Circularization and Stable Accretion

When the disrupted material moves around the central pulsar in an elliptical orbit with high ellipticity, dissipative processes, e.g. collisions, shocks, viscous dissipation, etc, will take effect (Shakura & Sunyaev 1973). These processes will convert some of the energy of the ordered bulk orbital motion into internal energy, part of which will be radiated and therefore lost from the gas. Thus the gas has to sink deeper into the potential of the central pulsar, orbiting it more closely. This in turn requires the gas to lose angular momentum. So, most of the disrupted material will spiral towards the central pulsar through a series of elliptical orbits with continuously decreasing ellipticities. The above process is called orbital circularization. During the circularization, some gas will move inwards due to the alpha viscosity process. In this study, as the corotation radius ($1.0 \times 10^8 \text{ cm}$) is smaller than the Alfvén radius ($7.0 \times 10^9 \text{ cm}$), the gaseous debris will first accumulate at the Alfvén radius of the pulsar. When the pressure exerted by the accreted material exceeds the magnetic pressure from the central pulsar, the gas will stream onto the poles of the pulsar along the magnetic field lines, changing the spin and emission properties of the central pulsar. After circularization, an accretion disk would be formed around PSR J0738–4042. The observed relatively stable spin-down rate at the last stage in Figure 1 (i.e., the Slowly Spinning-Down Phase) can be explained by the constant accretion from the disk. Comparing $\dot{\nu}$ in the Fast Spinning-Down Phase with that in the Slowly Spinning-Down Phase, we again get the difference as $\Delta(\dot{\nu}) = 0.16 \times 10^{-14} \text{ s}^{-2}$. This again gives the accretion rate as $\dot{m} = 6.0 \times 10^{12} \text{ g s}^{-1}$. During the accretion timescale, i.e. from September 2005 to now, the total accreted mass should be $1.2 \times 10^{21} \text{ g}$, which is consistent with the mass range of asteroids around neutron stars. In this study, we regard $1.2 \times 10^{21} \text{ g}$ as the lower limit of the mass of the asteroid.

The total time for the bound debris to complete the circularization process around the central compact object is (Ulmer 1999; Lu et al. 2006)

$$t_{\text{cir}} = n_{\text{orb}} T, \quad (7)$$

where n_{orb} is the number of orbits necessary for circularization, usually ranging between 2 and 10. For $T \sim 700$ days, we get $t_{\text{cir}} \sim 1400 - 7000$ days. It is interesting to note that in the $\dot{\nu} - t$ diagram (Fig. 1), beginning from September 2005, a total period of about 1800 days can be isolated, during which the curve shows noticeable variabilities before it finally enters the stable Slowly Spinning-Down Phase after about 2011. This time span is roughly consistent with the t_{cir} value that we derived, indicating that the circularization process was in progress in this period.

4 CONCLUSIONS AND DISCUSSION

In this study, by invoking an asteroid disrupted and accreted by PSR J0738–4042, we show that the pronounced change in the spin-down rate can be reasonably explained. In particular, the sudden initial reduction (i.e. the First Pulse in Fig. 1) of the spin-down rate comes from the initial accretion when the asteroid flies by the central pulsar for the first time, while the subsequent drop (the Drop in Fig. 1) is due to the bound gaseous debris flying away. The relatively stable spin-down rate at the last stage (the Slowly Spinning-Down Phase in Fig. 1) can be explained as the result of constant accretion from the transient accretion disk formed after the orbital circularization.

As suggested by Brook et al. (2014), we also expect the spin-down rate to return to its previous value when the material from the disrupted asteroid is exhausted. For a typical asteroid with a characteristic mass of 7.0×10^{21} g (and radius ~ 60 km), the disrupted material will be entirely swallowed by PSR J0738–4042 in a timescale of about $50(\frac{r}{60 \text{ km}})^3$ yr. However, notice that the mass range of the asteroid can extend from about 1.0×10^{10} g to $\sim 1.0 \times 10^{24}$ g, so the exact accretion time is quite uncertain. In the future, when the spin-down rate of PSR J0738–4042 returns to its previous value, we can use the accretion timescale to constrain the mass of the asteroid.

Huang & Geng (2014) proposed an external mechanism to explain the unprecedented anti-glitch observed in magnetar 1E 2259+586. In their model, the impact parameter is very small so that the solid body will collide with the neutron star before coming to the periastron. As their collision process is very fast and violent, a glitch and an associated hard X-ray burst will be produced. In our case, the encounter of the small body with the neutron star does not lead to a direct collision. It is a much gentler process, and also greatly prolonged. The change in the spin-down rate of PSR J0738–4042 comes from the tidal disruption and accretion of the asteroid, which is much longer and smoother compared with what happens in a direct collision. Therefore, mainly the spin-down rate of PSR J0738–4042 is affected and there is no obvious glitch induced.

The origin of the small body has been discussed in detail by Huang & Geng (2014). Observationally, pulsars may have planetary systems (Wolszczan 1994; Thorsett et al. 1999; Wang et al. 2006). So, first, asteroids could be scattered toward the central star due to the disturbance

of other planets (Guillochon et al. 2011). Second, comets in circumstellar Oort-like clouds may fall toward the central star after being disturbed by nearby stars (Tremaine & Zytkov 1986; Downs et al. 2013). Third, some clumps could be produced by the collision of planets in systems with multiple planets (Katz et al. 1994). Finally, a neutron star may encounter other stars with planetary systems due to its proper motion in space (Pineault & Poisson 1989).

In our calculations, the lower limit of the pericenter distance of the captured asteroid is estimated as $R_p = 1.9 \times 10^{10}$ cm, which is smaller than the tidal disruption radius ($R_t = 8.7 \times 10^{10}$ cm). In this case, named an ultra-close passage by Rees (1988), the asteroid will be completely disrupted. As discussed by Carter & Luminet (1982), such an asteroid is not only elongated along the orbital direction in the process, but will also undergo compression to form a short-lived pancake aligned in the orbital plane. They defined a factor β ($\beta \approx R_t/R_p$) to derive some key parameters in the case of an ultra-close passage. The maximum central temperature Θ_m and density ρ_m can be given by $\Theta_m = \beta^2 \Theta_*$ and $\rho_m = \beta^3 \rho_*$ respectively, where Θ_* and ρ_* are the central temperature and density of the asteroid in its unperturbed state. When $\beta \approx 10$, the temperature and density may rise enough to effectively detonate a significant fraction of the available thermonuclear fuel, which will affect the orbital evolution of the disrupted debris. In our case, β is only about 4, so we believe that the orbital motion and accretion process will not be significantly modified by this effect.

Acknowledgements This work was supported by the National Basic Research Program of China (973 Program, Grant No. 2014CB845800) and by the National Natural Science Foundation of China (Grant No. 11473012).

References

- Alpar, M. A., & Baykal, A. 2006, MNRAS, 372, 489
- Anderson, P. W., & Itoh, N. 1975, Nature, 256, 25
- Archibald, R. F., Kaspi, V. M., Ng, C.-Y., et al. 2013, Nature, 497, 591
- Backer, D. C. 1973, ApJ, 182, 245
- Bilous, A. V., Hessels, J. W. T., Kondratiev, V. I., et al. 2014, A&A, 572, A52
- Brook, P. R., Karastergiou, A., Buchner, S., et al. 2014, ApJ, 780, L31
- Burgay, M., Possenti, A., Manchester, R. N., et al. 2005, ApJ, 624, L113
- Şaşmaz Muş, S., Aydın, B., & Göğüş, E. 2014, MNRAS, 440, 2916
- Campana, S., Lodato, G., D’Avanzo, P., et al. 2011, Nature, 480, 69
- Carter, B., & Luminet, J. P. 1982, Nature, 296, 211
- Chamel, N. 2013, Physical Review Letters, 110, 011101
- Cognard, I., & Backer, D. C. 2004, ApJ, 612, L125
- Colgate, S. A., & Petschek, A. G. 1981, ApJ, 248, 771

- Deich, W. T. S., Cordes, J. M., Hankins, T. H., & Rankin, J. M. 1986, *ApJ*, 300, 540
- Dib, R., Kaspi, V. M., & Gavriil, F. P. 2009, *ApJ*, 702, 614
- Downs, C., Linker, J. A., Mikić, Z., et al. 2013, *Science*, 340, 1196
- Duncan, R. C., & Thompson, C. 1992, *ApJ*, 392, L9
- Esamdin, A., Lyne, A. G., Graham-Smith, F., et al. 2005, *MNRAS*, 356, 59
- Espinoza, C. M., Lyne, A. G., Stappers, B. W., & Kramer, M. 2011, *MNRAS*, 414, 1679
- Gavriil, F. P., Dib, R., & Kaspi, V. M. 2011, *ApJ*, 736, 138
- Ghosh, P., & Lamb, F. K. 1979a, *ApJ*, 232, 259
- Ghosh, P., & Lamb, F. K. 1979b, *ApJ*, 234, 296
- Glampedakis, K., & Andersson, N. 2009, *Physical Review Letters*, 102, 141101
- Guillochon, J., Ramirez-Ruiz, E., & Lin, D. 2011, *ApJ*, 732, 74
- Haskell, B., Pizzochero, P. M., & Sidery, T. 2012, *MNRAS*, 420, 658
- Hills, J. G. 1975, *Nature*, 254, 295
- Hooker, J., Newton, W. G., & Li, B.-A. 2015, *MNRAS*, 449, 3559
- Huang, Y. F., & Geng, J. J. 2014, *ApJ*, 782, L20
- Jones, P. B. 2011, *MNRAS*, 414, 759
- Jones, P. B. 2014, *MNRAS*, 437, 4027
- Karastergiou, A., Roberts, S. J., Johnston, S., et al. 2011, *MNRAS*, 415, 251
- Kaspi, V. M., Lackey, J. R., & Chakrabarty, D. 2000, *ApJ*, 537, L31
- Katz, J. I. 2014, *Ap&SS*, 349, 611
- Katz, J. I., Toole, H. A., & Unruh, S. H. 1994, *ApJ*, 437, 727
- Li, J., Esamdin, A., Manchester, R. N., Qian, M. F., & Niu, H. B. 2012, *MNRAS*, 425, 1294
- Livingstone, M. A., Kaspi, V. M., & Gavriil, F. P. 2010, *ApJ*, 710, 1710
- Livio, M., & Taam, R. E. 1987, *Nature*, 327, 398
- Lu, Y., Cheng, K. S., & Huang, Y. F. 2006, *ApJ*, 641, 288
- Lyutikov, M. 2013, arXiv:1306.2264
- Manchester, R. N., & Hobbs, G. 2011, *ApJ*, 736, L31
- Mandal, R. D. R., Konar, S., Dey, M., & Dey, J. 2009, *MNRAS*, 399, 822
- Morley, P. D., & Schmidt, I. 1996, *EPL (Europhysics Letters)*, 33, 105
- Olausen, S. A., & Kaspi, V. M. 2014, *ApJS*, 212, 6
- Ouyed, R., Leahy, D., & Koning, N. 2014, *Ap&SS*, 352, 715
- Page, C. G. 1973, *MNRAS*, 163, 29
- Pineault, S., & Poisson, E. 1989, *ApJ*, 347, 1141
- Pines, D., & Alpar, M. A. 1985, *Nature*, 316, 27
- Pizzochero, P. M. 2011, *ApJ*, 743, L20
- Poutanen, J., Ibragimov, A., & Annala, M. 2009, *ApJ*, 706, L129
- Rankin, J. M. 1986, *ApJ*, 301, 901
- Rankin, J. M., & Wright, G. A. E. 2008, in *American Institute of Physics Conference Series*, 983, 40 *Years of Pulsars: Millisecond Pulsars, Magnetars and More*, eds. C. Bassa, Z. Wang, A. Cumming, & V. M. Kaspi, 91
- Rees, M. J. 1988, *Nature*, 333, 523
- Ruderman, M. 1976, *ApJ*, 203, 206
- Seveso, S., Pizzochero, P. M., & Haskell, B. 2012, *MNRAS*, 427, 1089
- Shakura, N. I., & Sunyaev, R. A. 1973, *A&A*, 24, 337
- Shannon, R. M., Cordes, J. M., Metcalfe, T. S., et al. 2013, *ApJ*, 766, 5
- Thompson, C., Duncan, R. C., Woods, P. M., et al. 2000, *ApJ*, 543, 340
- Thorsett, S. E., Arzoumanian, Z., Camilo, F., & Lyne, A. G. 1999, *ApJ*, 523, 763
- Tremaine, S., & Zytkov, A. N. 1986, *ApJ*, 301, 155
- Ulmer, A. 1999, *ApJ*, 514, 180
- Usov, V. V. 1992, *Nature*, 357, 472
- van Buren, D. 1981, *ApJ*, 249, 297
- Wang, N., Manchester, R. N., Pace, R. T., et al. 2000, *MNRAS*, 317, 843
- Wang, Z., Chakrabarty, D., & Kaplan, D. L. 2006, *Nature*, 440, 772
- Warszawski, L., & Melatos, A. 2011, *MNRAS*, 415, 1611
- Warszawski, L., Melatos, A., & Berloff, N. G. 2012, *Phys. Rev. B*, 85, 104503
- Weltevrede, P., Johnston, S., Manchester, R. N., et al. 2010, *PASA*, 27, 64
- Wolszczan, A. 1994, *Science*, 264, 538
- Wu, X.-F., Hou, S.-J., & Lei, W.-H. 2013, *ApJ*, 767, L36
- Yu, M., Manchester, R. N., Hobbs, G., et al. 2013, *MNRAS*, 429, 688
- Yu, Y. B., Wu, X. F., Huang, Y. F., et al. 2015, *MNRAS*, 446, 3642
- Yuan, J. P., Manchester, R. N., Wang, N., et al. 2010, *ApJ*, 719, L111
- Zhang, B., Xu, R. X., & Qiao, G. J. 2000, *ApJ*, 545, L127
- Zhou, E. P., Lu, J. G., Tong, H., & Xu, R. X. 2014, *MNRAS*, 443, 2705